Area theorem for surface plasmons interacting with resonant atoms

Sergey A. Moiseev [1,*] and Ali A. Kamli [2,†]

[1]*Kazan Quantum Center, Kazan National Research Technical University n.a. A.N. Tupolev-KAI, 10 K. Marx St., Kazan 420111, Russia*
[2]*Department of Physics, Jazan University, Jazan Box 114, Saudi Arabia*

We show how the area theorem is applicable to the analytical description of the nonlinear interaction of surface plasmon modes with resonant two-level atoms. A closed analytical solution is obtained and analyzed for a dielectric-negative index metamaterial interface, which shows that surface plasmons can form long-propagating 2π pulses when interacting with an optically dense two-level atomic ensemble. The possible applications of the surface pulse area theorem and the conditions for the detection of 2π surface plasmon pulses are discussed.

I. INTRODUCTION

The resonant interaction of light pulses with coherent atomic ensembles plays an important role in quantum optics, laser physics, and quantum technologies [1–3]. Considerable advances have been achieved over the past years in cavity systems and photonic structures and, more recently, in the field of plasmonics. The surface plasmon (SP) modes propagate at the interface connecting a dielectric and metal with highly confined electric field amplitude and thus large energy concentration at nanoscale distances near the interface [4–7]. The nano-optics nature of these SP modes enables them to circumvent the diffraction limit that other techniques suffer, making plasmonics viable candidates to generate strong coupling with atoms and thus providing a potential platform to explore coherent light-atom interactions and possible device applications that require strong coupling with atoms. These properties of SP fields are of great interest for the coherent interaction of light with resonant atomic ensembles [8–14].

The highly inhomogeneous spatial structure of the electromagnetic field of SP greatly complicates the theoretical description of the nonlinear effects of their interaction with atoms. These difficulties are currently being overcome by the use of perturbation theory [10,11,13], which has a limited scope of applicability and does not allow a more complete understanding of the nonlinear patterns of the interaction of SP pulses with resonant atoms. In this paper, we want to draw attention to the usefulness of using the area theorem for the theoretical description of the nonlinear coherent interaction of SP pulses with resonant atoms.

The area theorem provides researchers with a powerful tool for obtaining exact analytical solutions of nonlinear equations [15] that allow the description of general patterns of interaction and propagation of light pulses in a coherent resonant medium. The area theorem was derived in the well-known work of McCall and Hahn [15] for the propagation of a light pulse through a resonant medium of two-level atoms, which led to the prediction of self-induced transparency for

light pulses having a pulse area equal to 2π, and then led to the discovery of optical solitons [16]. The pioneering theoretical and experimental work on area theorem [15] for the interaction of a single light pulse with resonant atoms has induced much work devoted to its application to solving various problems of the interaction of light pulses with resonant atomic ensembles. As an example, we note the application of the area theorem [15–18] to the photon echo in an optically dense medium [19–24], self-induced transparency [25] and photon echo [26] in resonators, and cavity-assisted Dicke superradiance [27], and to the description of the interaction of light pulses with three-level [28,29] and four-level atoms [30], optical quantum memory protocols [31,32], and the description of various modes of laser generation [33,34].

In this work, we develop the pulse area approach for SP modes interacting with an inhomogeneously broadened two-level atomic ensemble. For a more general analysis, we take the interface to contain a dielectric doped by the two-level atoms and a negative index metamaterial (NIMM) [35–37], since a NIMM interface supports both transverse electric (TE) and transverse magnetic (TM) polarized SP modes. The interest in these artificially fabricated materials has also expanded due to the fabrication of NIMMs at optical and desirable frequencies, and more recently on crystals with rare-earth ions at telecommunication wavelength [38], the emergence of quantum plasmonics, and the possibilities of implementing optical quantum processing (see reviews [39–43]).

The strong coupling of the SP modes with two-level atomic ensemble leads to nonlinear dynamics of SP modes propagation that we like to explore. Here, we are interested in the possibility of modifying the McCall-Hahn theorem and the formation of long-propagating 2π pulses in this case.

II. PLASMONIC MODES

In Fig. 1 we show the hybrid structure under consideration, containing a dielectric-metamaterial interface with an ensemble of two-level atoms. The upper half-space of the interface ($z > 0$) can be any dielectric material characterized by constant dielectric function or permittivity ε_1 and constant magnetic permeability μ_1. In the analysis below we shall take the upper half to be a rare-earth dielectric crystal. The

---

*Contact author: s.a.moiseev@kazanqc.org
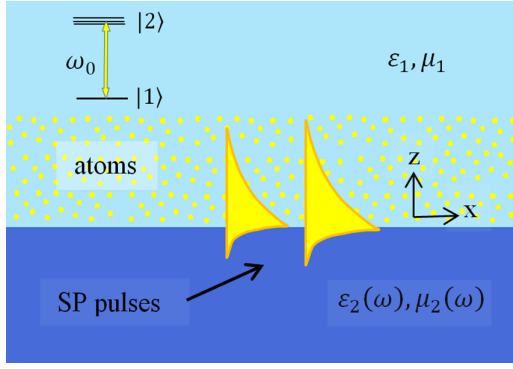†Contact author: alkamli@jazanu.edu.sa

FIG. 1. An interface containing a dielectric in the upper half-space ($z > 0$) with constant permittivity ε_1 and permeability μ_1 and a NIMM in the lower half-space ($z < 0$) characterized by a dielectric function $\varepsilon_2(\omega)$ and permeability $\mu_2(\omega)$. The two media are joined at interface $z = 0$. The electric field of the SP mode decreases exponentially with the distance z from the interface. The SP pulses propagate along the x direction, interacting with a two-level inhomogeneously broadened atomic ensemble (atomic states $|1\rangle$ and $|2\rangle$) located above the interface, where ω_0 is a central frequency of atomic transition and a carrier frequency of SP pulse.

two-level atoms are embodied in the dielectric crystal part of this structure with a given atomic density $\rho(x, y, z)$ and inhomogeneous broadening function $G(\Delta/\Delta_{\rm in})$ of resonant transition ($\Delta_{\rm in}$ - linewidth) and detuning Δ. The lower half-space of the interface ($z < 0$) is a NIMM medium characterized by frequency-dependent complex dielectric function or permittivity $\varepsilon_2(\omega)$ and complex magnetic permeability $\mu_2(\omega)$. For a certain frequency range, the real parts of $\varepsilon_2(\omega)$ and $\mu_2(\omega)$ are negative. When both real parts of $\varepsilon_2(\omega)$ and $\mu_2(\omega)$ are negative, both TE- and TM-polarized plasmonic modes can exist with low losses, and this is the main advantage of using NIMM in this work.

These SP modes are confined to interface and propagate in the x direction with complex wave vector $K_\parallel$. We shall assume that the propagation along the x direction is facilitated by a channel or groove [44] of width L_y in the y direction so as to direct the SP propagation along the x direction. We shall shortly estimate the width of this channel. The SP electric field amplitudes decay away in both sides with distance from the interface at $z = 0$ with high energy concentration close to interface. So, the SP electric field E of a transverse mode of frequency ω satisfying the wave equation

$$\nabla^2 E_m + \omega^2 \varepsilon_0 \mu_0 \, \varepsilon_m(\omega)\mu_m(\omega)E_m = 0 \qquad (1)$$

is in the form ($m = 1,2$ for the two media)

$$\mathbf{E_k}(\mathbf{r}) = e^{iK_\parallel x}\left[u(z)\left(\hat{\mathbf{x}} + \hat{\mathbf{z}}\frac{iK_\parallel}{k_1}\right)e^{-k_1 z}A_1 + u(-z)\right.$$
$$\left.\times\left(\hat{\mathbf{x}} - \hat{\mathbf{z}}\frac{iK_\parallel}{k_2}\right)e^{k_2 z}A_2\right]. \qquad (2)$$

Here, $u(z)$ is the Heaviside step function, and the constants $A_{1,2}$ are to be determined from boundary conditions and SP field quantization shortly. Where ε_0 is the vacuum dielectric constant (or permittivity) and μ_0 is the vacuum permeability, $c = 1/\sqrt{\varepsilon_0\mu_0}$ is the speed of light in vacuum, $\varepsilon_m(\omega)$

is the dielectric function of the medium, and $\mu_m(\omega)$ is magnetic permeability. The wave numbers $k_m \equiv k_m(\omega) = \sqrt{K_\parallel^2 - (\omega/c)^2\varepsilon_m(\omega)\mu_m(\omega)}$ are the wave vector components along the z direction normal to the interface characterized by positive real parts $\mathrm{Re}[k_m] > 0$ so that the SP field amplitudes decay away from the interface. These SP modes are thus bound to interface and propagate at wave vector $\mathbf{K}_\parallel$ parallel to the interface. Applications of electromagnetic boundary conditions at interface $z = 0$, namely, continuity of tangential electric fields, leads to $A_1 = A_2 = \mathcal{N}$, an overall normalization factor to be determined shortly. The continuity of displacement vector normal to interface results in the following condition for TM-polarized SP modes [5,6]:

$$k_1\varepsilon_2(\omega) + k_2\varepsilon_1(\omega) = 0,$$

$$K_\parallel = k_\parallel + i\kappa = \frac{\omega}{c}\sqrt{\varepsilon_1\varepsilon_2\frac{\mu_1\varepsilon_2 - \mu_2\varepsilon_1}{\varepsilon_2^2 - \varepsilon_1^2}}. \qquad (3)$$

The case of TE modes can be analyzed along the same line with the exchange $\varepsilon \leftrightarrow \mu$. In this work we focus on analysis for the TM modes, and shall drop reference to the mode index.

In these equations, the real part $k_\parallel$ of the complex wave vector $K_\parallel$ gives the dispersion relations for (TM-polarized) SP modes, while the imaginary part κ gives SP loss that determines the SP propagation distance $L_x = 1/|\kappa|$ along the interface. The positive real parts of the wave numbers k_m normal to interface give the skin or penetration depth of the fields into both media, which we take as our definition of field confinement and denote as $\zeta_m = 1/\mathrm{Re}[k_m]$. Smaller values of ζ_m indicate better confinement, which means the field can be confined to a dielectric interface, and vice versa; large ζ_m leads to poor confinement or possibly deconfinement. The SP propagation distance L_x and confinement ζ_m are interrelated, as we see shortly. Since real $k_{1,2}$ are positive, Eq. (3) is fulfilled when the electric permittivity of one of the two media has a negative real part.

To illustrate the basic dispersion and losses of these modes, we take the case where the first medium is described by the pair ($\mu_1 = 1$ and $\varepsilon_1 = 1.5$) corresponding to a crystal doped by rare-earth ions, while NIMM is modeled in the Drude model by the frequency-dependent electric permittivity $\varepsilon_2(\omega)$ and magnetic permeability $\mu_2(\omega)$ as

$$\varepsilon_2(\omega) = 1 - \frac{\omega_e^2}{\omega(\omega + i\gamma_e)}, \quad \mu_2(\omega) = 1 - \frac{\omega_h^2}{\omega(\omega + i\gamma_h)},$$
$$(4)$$

where ω_e is the electron plasma frequency usually in the ultraviolet region, γ_e is the electric damping rate due to material losses, ω_h is the magnetic plasma frequency, and γ_h is the magnetic damping rate. The plasma frequency ω_e is a natural scale for frequency and the corresponding plasma wave number $k_e = \omega_e/c$ is the scale for all wave numbers.

The dispersions are shown in Fig. 2, where we display the mode frequency ω/ω_e as a function of real part $k_\parallel$ scaled to k_e, and in Fig. 3 we show losses as given by $\kappa(\omega) = \mathrm{Im}[K_\parallel(\omega)]$ of Eq. (3) scaled to k_e. The parameters are $\omega_e = 1.4 \times 10^{16}s^{-1}$, $\gamma_e = 2.73 \times 10^{15}s^{-1}$ (for silver). Since the medium response to the magnetic component of the field is weaker than the electric component, we assume $\omega_h = \omega_e/2$ and $\gamma_h = \gamma_e/500$.
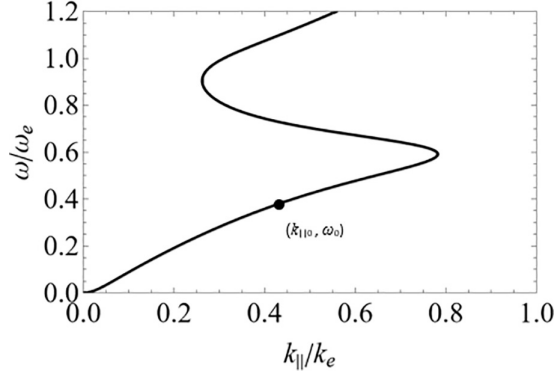
FIG. 2. Dispersion curves showing TM mode frequency ω/ω_e as a function of wave number $k_{||}/k_e$, $\omega_e = 1.4 \times 10^{16} s^{-1}$, $k_e = 4.5 \times 10^7 m^{-1}$. The point $(k_{||0}, \omega_0)$ scans the linear part of dispersion where ω_0 is the atomic ensemble central frequency and $k_{||0} = k_{||}(\omega_0)$. The linear segment in the lower branch of the curve is the part of interest to us.

From Fig. 2, the dispersion relation is approximately linear in the frequency range below $\omega/\omega_e < 0.35$, and losses measured in k_e are also highly reduced in this frequency range (Fig. 3). We note here that the frequency $\omega/\omega_e = 0.4$ is enticing to work with since it corresponds to highly reduced losses, which are, however, accompanied by very poor confinement and may even complete deconfinement. This trade-off between losses and confinement means we need to maintain a reasonable level of losses and SP field confinement in the chosen frequency range. So, for the rest of this work, we will focus on the frequency range $0.05 < \omega/\omega_e < 0.35$, where dispersion is linear, losses are reduced, and SP fields are confined, as our operating working frequency range.

We now estimate the required channel width L_y needed to direct SP propagation along the x direction by estimating the minimum uncertainty or deviation in the SP frequency ($\Delta\omega$) inside and outside the channel. The uncertainty in the SP energy is $\Delta E \Delta t \geqslant \hbar$, where $\Delta t \approx L_y/v_g$ is the time to traverse the channel width L_y at the surface plasmon group velocity v_g calculated from the dispersion relation. Then, the SP energy deviation is $\Delta E \geqslant \hbar v_g/L_y$. Taking the channel width of order 400 nm and $v_g \approx 0.8c$, the frequency deviation
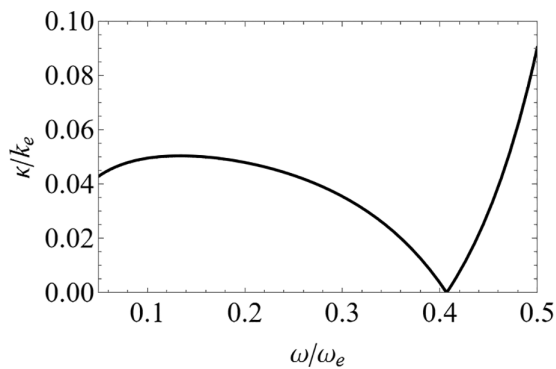

FIG. 3. SP losses $\kappa(\omega)$ scaled to plasma wave number k_e as given by the imaginary part of the SP wave vector are shown as a function of scaled mode frequency ω/ω_e. Parameters as in Fig. 2, and see also text.

corresponding to this energy deviation is $\Delta\omega = 0.5 \, eV/\hbar$. For SP modes (without the channel) the frequency is usually of the order of the plasma frequency $\omega_e = 1.4 \times 10^{16} \, s^{-1}$ (for silver, for example), and thus the SP energy is $E = \hbar\omega = 9.2$ eV. Then, for the channel width $L_y \approx 400$ nm, the frequency deviation is reduced by an amount $(0.5 \, eV/\hbar)/(9.2 \, eV/\hbar) \approx 5\%$. The frequency deviation is the difference between the SP frequency inside and outside the channel, so by taking the channel width of the order 400 nm, this frequency deviation can be reduced and made as small as 5%, which means that the width 400 nm is large enough to neglect the frequency deviation and assume the SP frequency inside and outside the channel are practically the same and ignore the channel edge effects.

III. QUANTIZED SP FIELDS

We adopt a quantum approach to substantiate the initial equations and for more general analysis of the interaction of SP fields with atomic ensemble. We are concerned here with SP transport along the x direction in optically dense atomic medium. In the low loss range ($0.05 < \omega/\omega_e < 0.35$) $K_{||} \approx k_{||} \equiv k$, and the SP quantization will determine the field amplitudes needed to couple to the two-level atoms that we need to consider in the next section. The quantized SP field is constructed as the sum of SP modes of the type in Eq. (2) and is written as

$$\hat{\mathbf{E}}(\mathbf{r}, t) = \int \mathbf{E}(k, z)\hat{a}(k, t)e^{ikx}dk + \text{H.c.}, \quad (5)$$

where we use shorthand notation $k = k_{||}$. The mode field operators $\hat{a}(k, t)$ and $\hat{a}^\dagger(k, t)$ of the plasmonic modes obey the bosonic equal time commutation relation $[\hat{a}(k, t), \hat{a}^\dagger(k', t)] = \delta(k - k')$.

The quantization procedure [7–9] culminates in the following expression for the SP field amplitude (see Appendix for details):

$$\mathbf{E}(k, z) = \mathcal{N}\left[u(z)\left(\hat{\mathbf{x}} + \hat{\mathbf{z}}\frac{ik}{k_1}\right)e^{-k_1 z} + u(-z)\left(\hat{\mathbf{x}} - \hat{\mathbf{z}}\frac{ik}{k_2}\right)e^{k_2 z}\right], \quad (6)$$

where

$$\mathcal{N}(\omega) = \sqrt{\frac{\hbar\omega}{2\pi\varepsilon_0 L_y L_z(\omega)}}, \quad (7)$$

$$L_z(\omega) = D(\omega) + \frac{\omega^2}{c^2}S(\omega), \quad (8)$$

$$D(\omega) = \frac{1}{2}\zeta_1 \text{Re}\left(\frac{\partial(\omega\varepsilon_1)}{\partial\omega}\right)[1 + (\zeta_1 k)^2] + \frac{1}{2}\zeta_2 \text{Re}\left(\frac{\partial(\omega\varepsilon_2)}{\partial\omega}\right)[1 + (\zeta_2 k)^2], \quad (9)$$

$$S(\omega) = \frac{1}{2}\zeta_1^3 \text{Re}\left(\frac{\partial(\omega\mu_1)}{\partial\omega}\right)|\varepsilon_1|^2 + \frac{1}{2}\zeta_2^3 \text{Re}\left(\frac{\partial(\omega\mu_2)}{\partial\omega}\right)|\varepsilon_2|^2. \quad (10)$$

In the above equations, the normalization factor $\mathcal{N}(\omega)$ determines the field amplitude and is given in terms of various

plasmonic parameters. To avoid cumbersome notations and for convenience, we suppress the frequency dependence and write $\zeta_{1,2} = \zeta_{1,2}(\omega)$, $\varepsilon_2 = \varepsilon_2(\omega)$, $\mu_2 = \mu_2(\omega)$, $k_{1,2} = k_{1,2}(\omega)$, $k = k_{||}(\omega)$, etc., with $\zeta_m = 1/\text{Re}[k_m]$. We shall retain the frequency dependence when appropriate. Furthermore, we write quantities above as functions of ω only since $k_{||}$ is also a function of ω. The normalization length $L_z(\omega)$ is given in terms of confinement ζ_m and is determined by the physical properties of the NIMM medium, such as by its permittivity's ε and permeability's μ, given above.

An important point to note in Eqs. (7)–(10) is that larger values of the wave numbers $\text{Re}[k_m]$ lead to smaller values for ζ_m and thus highly confined modes. Likewise, suppressed values of $\text{Re}[k_m]$ mean large values of ζ_m, indicating poor confinement and thus large value of L_z. In the frequency range where confinement is high, we see that losses are also high, leading to short SP propagation distances $L_x = 1/|\kappa|$, while for poor confinement losses are low and hence longer propagation distance. This trade-off between confinement and losses needs to be considered carefully so that we can find the optimal confinement with optimal losses that suit practical needs. Appropriate choice of materials, i.e., adjusting the pairs (ε_1, μ_1) and (ε_2, μ_2), can lead to a decrease in $L_z(\omega)$. The reduction of the interaction volume $[L_x L_y L_z(\omega)]$ considerably enhances the field amplitude, thus leading to strong atom-field coupling [45].

IV. SP PULSE INTERACTION WITH TWO-LEVEL ATOMIC ENSEMBLE

We here explore the resonant interaction of the SP pulse modes with an ensemble of two level atoms near a NIMM interface as shown in Fig. 1. Recent work has shown [46] that an atomic ensemble can emit energy into SP modes at least two orders of magnitude stronger than into free space modes. Therefore, only the SP modes are included in the Hamiltonian used in studies of coherent interaction of an atomic ensemble. The total Hamiltonian is given as

$$\hat{H} = \hat{H}_a + \hat{H}_f + \hat{H}_{\text{int}}, \tag{11}$$

with

$$\hat{H}_a = \frac{1}{2} \sum_j \hbar(\omega_0 + \Delta_j)\sigma_z^j, \tag{12}$$

$$\hat{H}_f = \frac{1}{2} \int dk\hbar\omega(k)[\hat{a}^\dagger(k)\hat{a}(k) + \text{H.c.}], \tag{13}$$

$$\hat{H}_{\text{int}} = -\frac{1}{2} \sum_j \int dk\hbar\mathcal{R}(z_j)\sigma_+^j\hat{a}(k)e^{ikx_j} + \text{H.c.}, \tag{14}$$

where $\hat{H}_a$ is the atomic ensemble Hamiltonian with central transition frequency ω_0 and detuning Δ_j for the jth atom that is inhomogeneously broadened by function $G(\frac{\Delta}{\Delta_{in}})$ with spectral width Δ_{in}, the two-level atom operators are raising $\sigma_+^j = |2_j\rangle\langle 1_j|$, lowering $\sigma_-^j = |1_j\rangle\langle 2_j|$ operators, and the inversion $\sigma_z^j = \frac{1}{2}(|2_j\rangle\langle 2_j| - |1_j\rangle\langle 1_j|)$, $\hat{H}_f$ is the SP field part with mode frequency $\omega(k)$ (where $\mathbf{k} = k\mathbf{e}_x$), and $\hat{H}_{\text{int}}$ is the dipole interaction Hamiltonian of the SP field with atoms in slowly varying envelope approximation, $\mathbf{r}_j = (x_j, y_j, z_j)$ is position of the jth atom, and $\hbar$ is the reduced Planck constant. The

atom-SP field coupling strength $\mathcal{R}(z_j) = 2\mathbf{d}_{21}^j \cdot \mathbf{E}(z_j, \omega_0)/\hbar$ is a function of atomic location along the z direction normal to the interface and atomic central frequency ω_0. The SP field amplitude is given by Eqs. (6)–(10), and $\mathbf{d}_{21}^j$ is the dipole moment of the atomic transition. The Hamiltonian $\hat{H}_{\text{int}}$ describes the interaction of atoms with SP pulses in so-called rotating wave approximation, which is valid for pulses with sufficiently long duration $\delta t_s \gg \lambda/c$ and weak coupling constant of the SP field with atoms.

The effect of inhomogeneous broadening of the atomic transition of atoms located near a metal interface (dielectric-metamaterial) was considered in the experimental work [47], where the influence of inhomogeneous broadening on the decay of atomic coherence excited by short pulses in interaction with surface plasmons was demonstrated. In addition, the presence of inhomogeneous broadening makes it possible to realize strong interaction of atoms (molecules) with SP modes [45] and implementation of photon echo on surface plasmons [48,49].

As a resonant two-level atomic ensemble we take an ensemble of rare-earth ions (REIs) in a crystal (like Eu^{3+} and Pr^{3+} ions in Y_2SiO_5 crystal). We assume, as it is the case, that the experiment is carried out at low (helium) temperatures ($T < 4.2$ K), when the inhomogeneous broadening of the resonant optical transition of REIs is due to the presence of the static local inhomogeneities of electric fields. A very characteristic property of the REIs at such temperatures is the relatively large value of the inhomogeneous broadening of optical transitions, which significantly exceeds the homogeneous linewidth γ ($\Delta_{\text{in}} \gg \gamma$) determined by the dipole-dipole interaction and the dynamic fluctuations of local fields [50]. In this case, the inhomogeneous broadening Δ_{in} usually lies in the range from 30 MHz to 10 GHz, while the homogeneous linewidth can be $\gamma \sim 50$ KHz and less [50]. More detailed information about coherent interactions of the light pulses with REIs in crystals at such temperatures can be found in recent reviews [51,52]. Furthermore, for the interaction of light and SP fields with REIs, the authors of the work [47,53] have shown that at small atomic concentration, the dipole-dipole interaction of REIs turns out to be so weak that it can be assumed that the electromagnetic field interacts individually with each atom. These properties correspond to the physical conditions of the system under consideration, which provide the possibility of applying the system of Maxwell-Bloch equations with the Hamiltonian (11), accordingly. It is also worth noting that a Hamiltonian similar to the one we use (11) has been recently applied in the studies of two-pulse photon echo on quantum emitters interacting with surface plasmons [48,49].

In the following we consider the interaction of a single short SP pulse with a system of resonant two-level atoms, which has a duration much shorter than the phase relaxation lifetime of atoms ($\delta t_s \ll \gamma^{-1} \sim T_2$). Regarding the atomic ensemble model we use, it should also be added that the optically excited atoms located very close to the interface of metal (metamaterial)-dielectric ($\lesssim 10$ nm) rapidly transmit their excitation to metal electrons in a nonradiative manner [53], so this small fraction of atoms will not participate in longer-term coherent interactions or may be removed during the interface fabrication process.

To explore the transport of SP fields in space, it is more appropriate to work in the Heisenberg picture with the SP field operator written in the space formalism. We define the space representation of SP field operators $\hat{a}(x, t)$ and its Hermitian conjugate $\hat{a}^{\dagger}(x, t)$ in terms of their Fourier transform operators $\hat{a}(k, t)$ and $(\hat{a}^{\dagger}(k, t) = [\hat{a}(k, t)]^{\dagger})$ by the relations

$$\hat{a}(x, t) = \frac{1}{\sqrt{2\pi}} \int_{-\infty}^{\infty} dk \hat{a}(k, t) e^{ikx},$$

$$\hat{a}(k, t) = \frac{1}{\sqrt{2\pi}} \int_{-\infty}^{\infty} dx \hat{a}(x, t) e^{-ikx}. \quad (15)$$

Furthermore, for the operators $\hat{a}(x, t)$ and $\sigma_{\pm}^{j}(t)$ we introduce the slowly varying operators $\tilde{a}(x, t), \tilde{\sigma}_{\pm}^{j}(t)$,

$$\hat{a}(x, t) = \tilde{a}(x, t) e^{-i(\omega_0 t - k_0 x)},$$

$$\sigma_{\pm}^{j}(t) = \tilde{\sigma}_{\pm}^{j}(t) e^{\pm i(\omega_0 t - k_0 x)}, \quad (16)$$

where $[\tilde{a}(x, t), \tilde{a}^{\dagger}(x', t)] = \delta(x - x')$, while $\sigma_{z}^{j}(t) = \tilde{\sigma}_{z}^{j}(t)$, and $k_0 \equiv k_{\|0} = k_{\|}(\omega_0)$ (see caption to Fig. 2). Then, the Heisenberg equation of motion for the operator $\hat{Q}(t)$,

$$i\hbar \frac{\partial \hat{Q}(t)}{\partial t} = [\hat{Q}(t), \hat{H}], \quad (17)$$

gives Heisenberg-Langevin equations of motion for the slowly varying field and atomic operators

$$\left(\frac{\partial}{\partial t} + \frac{\gamma_w}{2} + v_g \frac{\partial}{\partial x} \right) \tilde{a}(x, t)$$
$$= i\sqrt{\pi/2} \sum_j \mathcal{R}^*(z_j) \tilde{\sigma}_{-}^{j}(t) \delta(x - x_j) + \sqrt{\gamma_w} \hat{b}_{in}(x, t),$$
$$(18)$$

$$\frac{\partial \tilde{\sigma}_{-}^{j}(t)}{\partial t} = -i\Delta_j \tilde{\sigma}_{-}^{j}(t) - \frac{i}{2} \mathcal{R}(z_j) \sigma_{z}^{j}(t) \tilde{a}(x_j, t),$$

$$\frac{\partial \tilde{\sigma}_{z}^{j}(t)}{\partial t} = i[\mathcal{R}(z_j) \tilde{\sigma}_{+}^{j}(t) \tilde{a}(x_j, t) - \mathcal{R}^*(z_j) \tilde{\sigma}_{-}^{j}(t) \tilde{a}^{\dagger}(x_j, t)]. \quad (19)$$

The SP group velocity $v_g = \partial\omega/\partial k$ results from the expansion of $\omega(k) = \omega_0 + (k - k_0) \partial\omega/\partial k$, (with $k = k_{\|}$). In this expansion (see Fig. 2), $\omega_0 = \omega_k|_{k=k_0}$ corresponding to the two-level transition frequency center as in Fig. 1, and k_0 is the corresponding wave number on the dispersion relation; γ_w is a decay rate of the SP field, which will be discussed in connection with SP absorption coefficient; and $\hat{b}_{in}(x, t)$ is related to the local input Langevin force with the usual bosonic commutation rules ($[\hat{b}_{in}(x', t), \hat{b}_{in}^{\dagger}(x, t)] = \delta(x - x')$) and zero quantum average value $\langle \hat{b}_{in}(x, t) \rangle = 0$ [2].

V. SP AREA THEOREM

To proceed with the equations of motion in Eq. (19), we shall assume that the SP coherent field is represented by a coherent state whose eigenvalues are complex numbers so that we can replace the SP field operator by a complex quantity of some amplitude and phase. Furthermore, we consider only the situation of the large average number of quanta in the SP pulse, where the quantum correlations between SP field and atom operators can be ignored, and the average of product of

operators can be replaced by the product of averages [1], i.e.,

$$\langle \sigma_{z}^{j}(t) \tilde{a}^{\dagger}(x_j, t) \rangle \cong \langle \sigma_{z}^{j}(t) \rangle \langle \tilde{a}^{\dagger}(x_j, t) \rangle = S_{z}^{j}(t) b(x_j, t) e^{-i\varphi(x_j)},$$

$$\langle \sigma_{z}^{j}(t) \tilde{a}(x_j, t) \rangle \cong S_{z}^{j}(t) b(x_j, t) e^{i\varphi(x_j)},$$

where $\langle \sigma_{\pm,z}^{j}(t) \rangle = S_{\pm,z}^{j}(t)$, and $b(x, t)$ and $\varphi(x)$ are the SP (real value) field amplitude and phase.

Now, to calculate the macroscopic response in (18) for $\tilde{a}(x, t)$ we replace summation with integration as follows:

$$\sum_j \mathcal{R}^*(z_j) S_{-}^{j}(t) \delta(x - x_j)$$

$$= \int_0^{\infty} dz \int_0^{L_y} dy \rho(\mathbf{r}) \int_{-\infty}^{\infty} d\Delta G\left(\frac{\Delta}{\Delta_{in}}\right) \mathcal{R}^*(z) S_{-}(\Delta, \mathbf{r}, t), \quad (20)$$

where instead of the discrete variables $j, \Delta_j, \mathbf{r}_j$, we introduced continuous variables in the atomic coherence $S_{-}^{j}(t, \mathbf{r}_j) \to S_{-}(\Delta, \mathbf{r}, t)$. We consider only the symmetrical smooth shape of the inhomogeneous broadening $G(\frac{\Delta}{\Delta_{in}})$. This simplification is valid for a fairly narrow spectrum of the signal pulse $\delta\omega_s < \Delta_{in}$, the central frequency of which coincides with the center of resonance line $\omega_s = \omega_0$ [1]. The presence of any narrow resonant lines and branch cuts located at a great distance from the center of atomic transition will only affect the magnitude of the phase and group velocity of the SP field, which can be taken into account in the developed theoretical approach without leading to a qualitative change in the final result. In (20) $\rho(\mathbf{r})$ is the atomic density, which is assumed to be constant [$\rho(\mathbf{r}) = \rho_0 = N/V$], N is the total number of atoms, and V is the volume of the dielectric medium. In the above integration, we show explicitly the dependence of atomic coherence $S_{-}(\Delta, \mathbf{r}, t)$ on frequency detuning Δ, spatial position (x, z), and time t. Equation (20) means that there is a sufficiently large number of REIs $\delta N \gg 1$ in the volume $\delta V \approx \lambda^3$, the frequency distribution usually described by the spectrally broadened function $G(\frac{\Delta}{\Delta_{in}})$ at helium temperatures [50]. The dipole moments of optical transitions in REIs are two to three orders of magnitude weaker than in atoms with allowed optical transitions, which makes it possible to use a larger concentration of such ions and facilitate the feasibility of the model used (20).

It is clear from Eqs. (19) and (20) that the pulse transport properties are determined from the spatial shape of atomic density $\rho(\mathbf{r})$ and z dependence of the coupling strength $\mathcal{R}(z)$ at $y = 0$, which has position and mode frequency dependence (suppressed so far). To describe the atomic response to the action of a SP pulse, we take into account a negligibly small value of the homogeneous linewidth $\Delta_j \to \Delta_j - i\gamma$ where $\Delta_{in}, \delta t_s^{-1} \gg \gamma \to 0$ in the calculation of the envelope area $\eta(x, t) = \int_{-\infty}^{t} b(x, t)dt$. Integrating the first equation in (19) for SP pulse $\langle \tilde{a}(x, t) \rangle = b(x, t) e^{i\varphi(x)}$ in time $\int_{-\infty}^{\infty} dt \cdots$ and assuming all atoms initially in their ground states, $S_{-}(\Delta, x, z, -\infty) = 0$, so we get

$$\left(\frac{\partial}{\partial x} + \frac{\gamma_w}{2v_g} \right) \eta(x) e^{i\varphi(x)}$$

$$= \pi \frac{\sqrt{\pi/2}}{v_g} L_y G(0) \int_0^{\infty} dz \rho_0 |\mathcal{R}(z)|^2 \int_{-\infty}^{\infty} dt b(x, t)$$

$$\times e^{i\varphi(x)} S_z(\Delta = 0, x, z, t), \quad (21)$$

where we put the atomic coherence equal to its value in the center of the system $(y = 0)$ $S_z(\Delta = 0, \mathbf{r}, t) = S_z(\Delta = 0, x, y = 0, z, t) \equiv S_z(\Delta = 0, x, z, t)$, $\eta(x) = \int_{-\infty}^{\infty} b(x, t)dt$. When calculating the last integral on Δ in (20), we take into account that $G(\frac{\Delta}{\Delta_{\text{in}}}) = G(-\frac{\Delta}{\Delta_{\text{ig}}})$, $S_z(\Delta, \mathbf{r}, t) = S_z(-\Delta, \mathbf{r}, t)$, and the following property of Langevin forces $\int_{-\infty}^{\infty} \langle \hat{b}_{\text{in}}(x, t) \rangle dt = 0$ [2].

From the solution of (19) for $S_z(\Delta = 0, x, z, t) = -\cos[|\mathcal{R}(z)|\eta(x, t)]$ [where $S_z(0, x, z, -\infty) = -1$ at initial conditions] we obtain for Eq. (21)

$$\left(\frac{\partial}{\partial x} + \frac{\gamma_w}{2v_g}\right)\eta(x)e^{i\varphi(x)} = \pi\sqrt{\frac{\pi}{2}}\frac{G(0)L_y}{v_g}e^{i\varphi(x)}F[\eta(x)], \quad (22)$$

where

$$F[\eta(x)] = -\int_0^{\infty} dz\rho_0|\mathcal{R}(z)|\sin[|\mathcal{R}(z)|\eta(x)]. \quad (23)$$

We see that $\varphi(x) = $ Const is a solution of (22). The integration in Eq. (23) is evaluated over the cross section (y-z plane) normal to the field propagation direction x. The integral over z is evaluated by substituting the position-dependent coupling strength given from the SP field relations (6)

$$\mathcal{R}(z) = \mathcal{R}(z, \omega_0) = \mathcal{R}_0 e^{-k_1(\omega_0)z},$$

$$\mathcal{R}_0 = 2\frac{\mathcal{N}(\omega_0)}{\hbar}\left(d_x + \mathrm{i}d_z\frac{k(\omega_0)}{k_1(\omega_0)}\right), \quad (24)$$

where for short we write $\mathcal{R}_0 = \mathcal{R}(z = 0, \omega_0)$, and on resonance $\omega = \omega_0$. The dipole moment of atomic transition is $\mathbf{d}_{21} = \hat{\mathbf{x}}d_x + \hat{\mathbf{y}}d_y + \hat{\mathbf{z}}d_z$, and the atom SP-field interaction takes place above the interface in medium 1. The coupling strength is composed of components parallel d_x and normal d_z to interface with modulus $|\mathcal{R}_0|$.

Now, taking into account the constant atomic density $\rho(\mathbf{r}) = \rho_0$, and substituting from (24) for the coupling strength $\mathcal{R}(z)$ into (23) and evaluating the integration over z, Eq. (22) reduces to

$$\left(\frac{\partial}{\partial x} + \frac{\gamma_w}{2v_g}\right)\Theta(x) = -\alpha\frac{\sin^2[\Theta(x)/2]}{\Theta(x)}, \quad (25)$$

where the pulse area $\Theta(x) = |\mathcal{R}_0|\eta(x)$ and absorption coefficient α

$$\alpha = \frac{1}{2}\sqrt{\frac{\pi}{2}}\frac{\omega_0\rho_0 G(0)\big[d_x^2 + d_z^2(\zeta_1 k)^2\big]}{\epsilon_0\hbar}\frac{\zeta_1}{L_z v_g}. \quad (26)$$

The strong interaction of SP pulse with resonant atoms $(\alpha \gg \gamma_w/v_g)$ allows a closed analytical solution of (25), which gives finally the closed expression for the surface plasmonic pulse area theorem:

$$x = x_0 - \frac{1}{\alpha}\left(T\left[\frac{\Theta(x)}{2}\right] - T\left[\frac{\Theta(x_0)}{2}\right]\right), \quad (27)$$

where

$$T[y] = \ln[\sin(y)] - y\cot(y). \quad (28)$$

The "surface plasmonic area theorem" (SP area theorem) as given by Eq. (25) and its solution in Eqs. (27) and (28) are the main results here. Equation (25) is nonlinear like all other area theorems, and in NIMM it has a very rich spectrum of
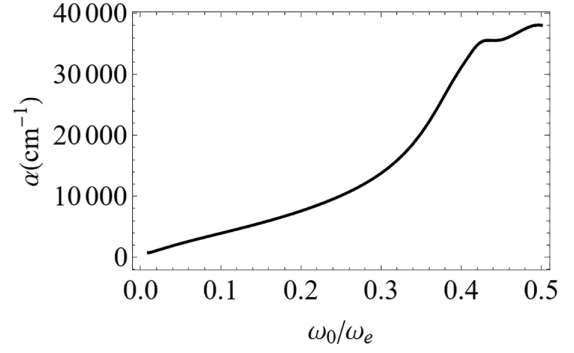

FIG. 4. The absorption coefficient as given by Eq. (26) as a function of atomic central frequency ω_0/ω_e, for REIs with the following parameters: atomic density $\rho_0 = 10^{25} \text{ m}^{-3}$, dipole moment of resonant transition $d = 5 \times 10^{-32} \text{ C m}$, inhomogeneous broadening $\Delta_{\text{in}} = 0.5 \times 10^8 \text{ s}^{-1}$.

structure parameters that can be utilized to explore its different facets; the modified pulse area $\Theta(x) = |\mathcal{R}_0|\eta(x)$ depends, among many parameters, on the SP modes confinement ζ_1, the SP group velocity v_g, the normalization length $L_z(\omega_0)$, and the modulus of the coupling strength $|\mathcal{R}_0|$. In the limit of a small pulse area $[\Theta(x_0) \ll \pi]$, Eqs. (25) and (27) reduce to the well-known Beer-Lambert law $[\Theta(x) = \Theta(x_0)e^{-\frac{\alpha}{2}(x-x_0)}]$. It is worth noting that due to the linearity of the quantum equations (19) when interacting with weak SP fields, this law (exponential decay of the fields) is obtained theoretically with a strict quantum approach to the SP field. In the case of a large pulse area, when nonlinear patterns of interaction between the SP field and atoms begin to appear, the influence of the quantum properties of the SP field remain an unsolved problem requiring special consideration.

VI. DYNAMICS OF 2π SP PULSES

The SP pulse dynamics is influenced by atomic and structure parameters. Equation (26) shows that the specific features of the absorption coefficient α, which are related to the interface properties, are determined by the multiplier $\beta(\omega_0) = \omega_0\zeta_1[1 + (\zeta_1 k)^2]/[L_z(v_g/c)]$, indicating that the maximum absorption gain occurs at a higher ratio of parameters $\frac{\zeta_1}{L_z}$ and lower group velocity v_g. At the same time, it is desirable to ensure this condition for a sufficiently high SP confinement (i.e., for a small value ζ_1). Using conservative spectroscopic parameters for the system of rare-earth ions, in Fig. 4 we plot the absorption coefficient $\alpha(\omega_0)$ as in Eq. (26) as a function of scaled central frequency ω_0/ω_e. The absorption coefficient obviously depends on the atomic part, namely, atomic density ρ_0, magnitude of dipole moment d, and the inhomogeneous broadening function $G(0)$, and on the NIMM part as given by the combined effects of the quantity $\beta(\omega_0)$. The qualitative behavior of the absorption is well represented by the combined effects of these parameters. However, its magnitude is influenced most by the atomic density, magnitude of dipole moment, and function $G(0)$.

The experimental data [50] for rare-earth ions give atomic concentration of $\rho_0 \approx 10^{25} \text{ m}^{-3}$, dipole moment $d \approx 5 \times 10^{-32} \text{ C m}$, and linewidth of optical transition $G(0) \approx \frac{1}{\Delta_{in}} =$
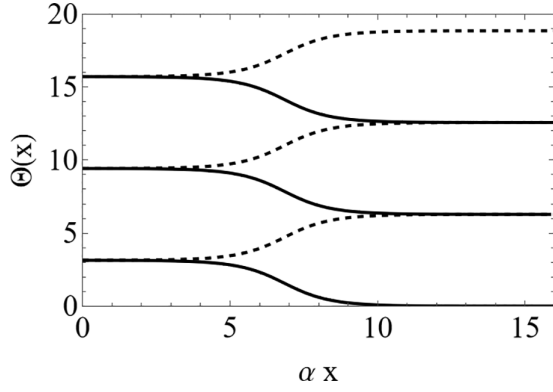
FIG. 5. The McCall-Hahn area theorem [Eq. (29)] [15] is shown for initial conditions $\Theta(x_0) = 0.9\pi, 2.9\pi, 4.9\pi$ (solid line) and $\Theta(x_0) = 1.1\pi, 3.1\pi, 5.1\pi$ (dotted line).

2×10^{-8} s. For this set of parameters we get $\alpha \approx 40\,000$ cm^{-1} for the frequency range of interest. It is possible to achieve a higher optical depth α by choosing crystals with less inhomogeneous broadening and a higher concentration of rare-earth ions [38]. With such a value for the resonance absorption coefficient α, we can see from Eq. (25) that the SP decay rate γ_w is negligibly small compared with α when $\gamma_w/v_g < 4000$ cm^{-1}, which is often implemented experimentally [5]. It is worth noting that the absorption coefficient of surface plasmons can be significantly lower in a number of materials, for example, in graphene [54], which will significantly simplify the feasibility of the condition $\alpha \gg \gamma_w/v_g$ for the implementation of the considered interaction of SP fields with resonant atoms. In the studied frequency range, the spatial localization of surface plasmons near the interface is about $\zeta_{1,\max} \cong 500$ nm. For the validity of using the SP area theorem, the resonant atoms must be also located in a layer (see Fig. 1) approximately no less than $\sim 3\zeta_{1,\max}$.

The possibility of increasing resonant absorption by using a higher atomic concentration requires special consideration in order to take into account the influence of interatomic interactions on the growth of the atomic phase relaxation in the hybrid system under consideration. It is worth noting that the pulse area $\Theta(x)$ in the SP area theorem is determined by the maximum of SP amplitude, which takes place near the interface surface. Accordingly, the enhanced interaction of the SP field with resonant atoms is directly affected by the increase in the optical density of the resonant transition.

It is interesting to compare the properties of the SP area theorem and the McCall-Hahn area theorem [15,17,18] derived for the case of the interaction of a light pulse with two-level atoms in a free space, which has the general solution

$$x = x_0 - \frac{1}{\alpha} \ln\left(\frac{\tan[\Theta(x)/2]}{\tan[\Theta(x_0)/2]} \right). \tag{29}$$

In Figs. 5 and 6 we compare the two area theorems as given by Eqs. (27) and (29) for the same initial pulse areas. As can be seen in both cases, the evolution of the pulse areas of the input signals leads to the formation of $2n\pi$ pulses propagating over long distances in an optically dense medium. At the same time, there are significant differences in the dynamics of the formation of these 2π pulses in these two cases. In
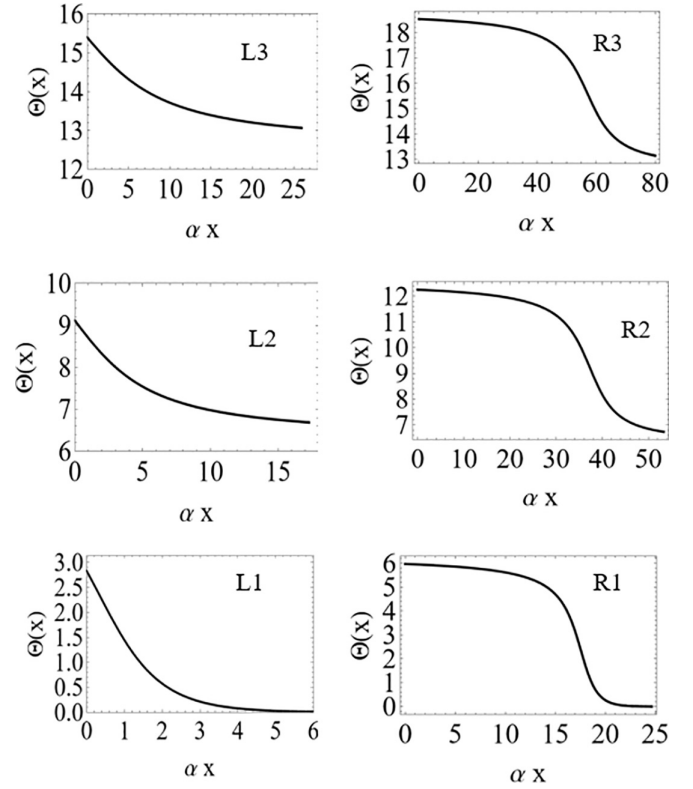

FIG. 6. The SP area theorem [Eq.(27)] for the initial conditions (L1) $\Theta(x_0) = 0.9\pi$, (L2) 2.9π, (L3) 4.9π, (R1) 1.98π, (R2) 3.98π, and (R3) 5.98π.

contrast to the solution of the McCall-Hahn area theorem [15], the SP area theorem does not have the bifurcation points $\Theta(x_0) = (2n+1)\pi$. In addition, the arising 2π SP pulses are unstable: even with a slight decrease in the pulse area relative to $2n\pi$ [$\Theta(x_0) = 2n\pi - \epsilon, \epsilon \ll 1$], its subsequent evolution leads to the state $\Theta(x \to \infty) \to 2(n-1)\pi$, as seen in Fig. 6. Taking into account the irreversible losses in accordance with (25), the attenuation rate of $\Theta(x)$ near $\sim 2n\pi$ is equal to $\frac{\partial}{\partial x}\Theta(x) \approx -n\pi\gamma_w/v_g$ and is enhanced with increasing the losses parameter γ_w/v_g and number of 2π pulses.

Moreover, in contrast to the formation of 2π pulses (solitons) in free space, an increase in the total pulse area of the input SP pulse $\Theta(0) > 2n\pi$ ($n > 2, 3, \ldots$) lengthens the formation time of independent 2π SP pulses. It seems unlikely that the 2π SP pulse propagates in an optically dense medium while maintaining its temporal shape. The SP area theorem does not provide information about the temporal shape of 2π SP pulses and the dynamics of their creation from the input intense SP pulse in the medium. The analysis of this issue is beyond the scope of this work. Elucidation of the space-time structure of such 2π SP pulses and the features of their interaction with a resonant atomic ensemble will allow us to understand the characteristic properties of their occurrence and propagation over long distances.

VII. DISCUSSION AND CONCLUSION

In this work we derived the pulse area theorem for the resonant interaction of SP pulse with a two-level

inhomogeneously broadened atomic ensemble and obtained its closed analytical solution. The SP area theorem predicts long propagating 2π SP pulses. The analysis has been performed for TM-polarized SP modes on the interface of a dielectric crystal doped by rare-earth ions with NIMM medium, and it is valid also for TE-polarized SP modes due to the same spatial properties (exponential shape) of the electromagnetic field of SP field magnitude in the dielectric part. Moreover, due to the same spatial property, the SP area theorem can be applied to the SP modes interacting with resonant atoms on the dielectric-metal interface.

We have analyzed the physical conditions necessary to create 2π SP pulses propagating over long distances. We also note that in spite of significant differences in physical properties, Eq. (25) of the SP area theorem resembles the pulse area theorem in a single-mode optical waveguide [32]. The qualitative behaviors of the two cases may be traced back to the fact that both pulses have decaying field amplitudes that enter into the pulse areas. However, for the single waveguide pulses [32] the decay has the form of a Gaussian or Bessel function of the first kind, whereas for SP pulses decays are exponential, and the nature of these decays demonstrates the significance differences between the two cases. However, this resemblance in the theoretical description makes it possible to uniformly describe various effects of nonstationary nonlinear coherent interaction of structured light pulses and SP fields with resonant atomic ensembles. Herein, due to the strong interaction of the SP mode with resonant atoms, the formation of 2π SP pulses will be detected experimentally at an atomic concentration lower than in the case of the formation of optical solitons in a resonant medium [1,15,16,18].

It is worth noting that, unlike the very different behavior of the electromagnetic field of light modes in the cross section of various optical waveguides, the electromagnetic field of SP fields usually decreases exponentially with distance from the interface. This circumstance makes the SP area theorem important for describing the resonant interaction of atoms with SP fields not only on NIMMs, but also on the noble metals and other materials. Graphene may be particularly interesting due to the very low attenuation of SP fields and the large compactness of the devices being created. We believe the 2π SP pulses with their interesting properties outlined above are useful for further theoretical studies and experimental investigations.

We anticipate the SP area theorem can be helpful for studies of resonant interaction of SP pulse with resonant two- and multilevel atoms, and various effects such as Dicke superradiance of SP fields [55,56], SP lasing [57,58], description of SP echo effect [48,49] in optically dense media and SP echo spectroscopy of atoms on the surface, and microscopic transport of information via SP fields [47], all of which deserve independent research. In a recent paper [59], the authors also showed the possibility of implementing optical devices using a variety of atoms interacting with a surface plasmon polariton. In this regard, considering the possibility of implementing photon echo on surface plasmons [48,49], integrated circuits of quantum memory using photon echo on surface plasmons may be of interest [60].

The quantum approach developed here for the resonant interaction of SP fields with atoms made it possible to clarify the transition to solvable semiclassical equations and to relate the resulting solutions to limiting quantum cases. This approach can also be used to study other problems of quantum plasmonics related to the interaction of quantum and classical SP fields with two- and three-level atomic ensembles. In particular, it is for the quantum memory protocols where we usually need to describe the interaction of weak quantum and intensive light pulses with resonant atoms [32]. Although a complete quantum description of the area theorem does not yet exist, the proposed approach will be a useful guide for searching for further development of this theorem when studying the weak manifestation of the quantum nature of SP fields. Alongside this, the work of Hughes [61] shows that the area theorem for the interaction of light pulses with resonant atoms in free space becomes of limited validity when the temporal duration of classical light pulses becomes close to the period of the light wave, leading to deviation from the rotating wave approximation. However, a similar analysis of how the transition to a short SP pulse could impose restrictions on the applicability of the SP area theorem deserves special study elsewhere.

ACKNOWLEDGMENTS

APPENDIX: SP FIELD QUANTIZATION

Quantization of SP modes on dielectric-metal interface is discussed in Ref. [7], where the authors use quantization of a discrete set of SP modes. In our case, to describe the interaction of a SP pulse with an atomic ensemble, it is more convenient to use a continuous set of SP modes. We start from the electromagnetic field energy in a dispersive medium [62] as

$$H_{\text{field}} = \frac{1}{2} \int d^3 r [\tilde{\varepsilon} |\hat{\mathbf{E}}(r)|^2 + \tilde{\mu} |\hat{\mathbf{H}}(r)|^2], \qquad \text{(A1)}$$

$$\tilde{\varepsilon} = \text{Re}\left[\frac{\partial}{\partial \omega}(\omega \varepsilon_0 \varepsilon(\omega))\right], \quad \tilde{\mu} = \text{Re}\left[\frac{\partial}{\partial \omega}(\omega \mu_0 \mu(\omega))\right]. \qquad \text{(A2)}$$

The SP modes propagate along the x direction with a wave number $k_{||}$. The electric field operator is constructed as a sum of modes, which we write as

$$\hat{\mathbf{E}}(r, t) = \int dk_{||} \mathbf{E}(k_{||}, z) \hat{a}(k_{||}) e^{i(k_{||}x - \omega t)} + \text{H.c.}, \qquad \text{(A3)}$$

The corresponding magnetic field operator $\mathbf{H}(r, t)$ is determined from Maxwell curl equation $i\omega\mu_0 \mathbf{H} = \text{curl}\mathbf{E}$, and given as

$$\hat{\mathbf{H}}(r, t) = \int dk_{||} \mathbf{H}(k_{||}, z) \hat{a}(k_{||}) e^{i(k_{||}x - \omega t)} + \text{H.c.} \qquad \text{(A4)}$$

The plasmonic modes annihilation and creation operators $\hat{a}(k_{||})$ and $\hat{a}^\dagger(k_{||})$ of the (TM polarized) mode and wave vector $k_{||}$ obey the usual equal time commutation relation $[\hat{a}(k_{||}), \hat{a}^\dagger(k'_{||})] = \delta(k_{||} - k'_{||})$. The (TM) mode structure

functions satisfying the wave equation are

$$\mathbf{E}(k_{||}, z) = \mathcal{N}\left[u(z)\left(\hat{x} + i\hat{z}\frac{k_{||}}{k_1}\right)e^{-k_1 z} + u(-z)\left(\hat{x} - i\hat{z}\frac{k_{||}}{k_2}\right)e^{k_2 z}\right], \tag{A5}$$

$$\mathbf{H}(k_{||}, z) = \hat{y}\mathcal{N}\left[u(z)\frac{\varepsilon_0\varepsilon_1\omega}{ik_1}e^{-k_1 z} - u(-z)\frac{\varepsilon_0\varepsilon_2\omega}{ik_2}e^{k_2 z}\right], \tag{A6}$$

where $u(z)$ is the step function. The SP field normalization factor $\mathcal{N}$ is determined by the requirement that the field Hamiltonian in dispersive medium (A1) reduces to the canonical form Hamiltonian

$$H_{\text{field}} = \frac{1}{2}\int dk_{||}\hbar\omega(k_{||})[\hat{a}(k_{||})\hat{a}^\dagger(k_{||}) + \text{H.c.}]. \tag{A7}$$

Now we use the fields in Eqs. (A3)–(A6) into the Hamiltonian (A1) to evaluate the space integrals,

$$H_{\text{field}} = \frac{1}{2}\iint dxdy\int_0^\infty dz(\tilde{\varepsilon}_1|\hat{E}(z>0)|^2 + \tilde{\mu}_1|\hat{H}(z>0)|^2) + \frac{1}{2}\iint dxdy\int_{-\infty}^0 dz(\tilde{\varepsilon}_2|\hat{E}(z<0)|^2 + \tilde{\mu}_2|\hat{H}(z<0)|^2), \tag{A8}$$

where integration over the upper half-plane of Eq. (A8) gives

$$I_{E1} = \frac{1}{2}\iint dxdy\int_0^\infty dz\tilde{\varepsilon}_1|\hat{E}(z>0)|^2$$

$$= \frac{1}{2}\int dk_{||}dk'_{||}\tilde{\varepsilon}_1|\mathcal{N}|^2\hat{a}(k_{||})\hat{a}^\dagger(k'_{||})\left(1 + \frac{k_{||}k'_{||}}{k_1 k_1^*}\right)\int_0^{L_y}dy\int_0^\infty dze^{-2\text{Re}(k_1)z}\int_{-\infty}^\infty dxe^{i[(k_{||}-k'_{||})x-(\omega-\omega')t]} + \text{H.c.} \tag{A9}$$

The z integral gives confinement $\zeta_1 = 1/\text{Re}[k_1]$ and the integral over x gives $2\pi\delta(k_{||} - k'_{||})$, which we use to evaluate the $k_{||}$ integration that leads finally to the expression

$$I_{E1} = \frac{1}{2}\varepsilon_0\int dk_{||}[\hat{a}(k_{||})\hat{a}^\dagger(k_{||}) + \hat{a}^\dagger(k_{||})\hat{a}(k_{||})](2\pi L_y)\frac{1}{2}\zeta_1|\mathcal{N}|^2\text{Re}\left(\frac{\partial[\omega\varepsilon_1(\omega)]}{\partial\omega}\right)[1 + (\zeta_1 k_{||})^2]. \tag{A10}$$

The term $I_{E2} = (1/2)\int dxdy\int dz\tilde{\varepsilon}_2|\hat{E}(z<0)|^2$ in Eq. (A8) gives a similar expression with exchange 1 and 2, namely, $I_{E2} = I_{E1}(1 \leftrightarrow 2)$. Adding these two terms gives the electric part of energy,

$$I_E = \frac{1}{2}\varepsilon_0\int dk_{||}[\hat{a}(k_{||})\hat{a}^\dagger(k_{||}) + \hat{a}^\dagger(k_{||})\hat{a}(k_{||})](2\pi L_y)|\mathcal{N}|^2 D(\omega), \tag{A11}$$

$$D(\omega) = \frac{1}{2}\zeta_1\,\text{Re}\frac{\partial[\omega\varepsilon_1(\omega)]}{\partial\omega]}[1 + (\zeta_1 k_{||})^2] + \frac{1}{2}\zeta_2\text{Re}\frac{\partial[\omega\varepsilon_2(\omega)]}{\partial\omega}[1 + (\zeta_2 k_{||})^2]. \tag{A12}$$

The magnetic parts of energy given by the second and fourth terms in Eq. (A8) can be calculated in the same way, leading to

$$I_H = \frac{1}{2}\varepsilon_0\int dk_{||}[\hat{a}(k_{||})\hat{a}^\dagger(k_{||}) + \hat{a}^\dagger(k_{||})\hat{a}(k_{||})](2\pi L_y)|\mathcal{N}|^2\frac{\omega^2}{c^2}S(\omega), \tag{A13}$$

$$S(\omega) = \frac{1}{2}\zeta_1^3\text{Re}\frac{\partial[\omega\mu_1(\omega)]}{\partial\omega}|\varepsilon_1|^2 + \frac{1}{2}\zeta_2^3\text{Re}\frac{\partial[\omega\mu_2(\omega)]}{\partial\omega}|\varepsilon_2|^2. \tag{A14}$$

The total field Hamiltonian in dispersive medium Eq. (A8) is then obtained as

$$H_{\text{field}} = \frac{1}{2}\int dk_{||}[\hat{a}(k_{||})\hat{a}^\dagger(k_{||}) + \hat{a}^\dagger(k_{||})\hat{a}(k_{||})]2\pi\varepsilon_0 L_y L_z|\mathcal{N}|^2, \tag{A15}$$

$$L_z(\omega) = \left[D(\omega) + \frac{\omega^2}{c^2}S(\omega)\right]. \tag{A16}$$

This Hamiltonian reduces to the canonical Hamiltonian equation (A7) when

$$2\pi\varepsilon_0 L_y L_z(\omega)|\mathcal{N}(\omega)|^2 = \hbar\omega, \tag{A17}$$

which is Eq. (7), and we write all quantities as functions of mode frequency ω only since $k_{||}$ is also a function of ω.

[1] L. Allen and J. Eberly, *Optical Resonance and Two-Level Atoms*, Dover Books on Physics and Chemistry (Dover, New York, 1975), p. 256.

[2] M. O. Scully and M. S. Zubairy, *Quantum Optics* (Cambridge University, Cambridge, 1997).

[3] N. Sangouard, C. Simon, H. de Riedmatten, and N. Gisin, Quantum repeaters based on atomic ensembles and linear optics, Rev. Mod. Phys. **83**, 33 (2011).

[4] W. L. Barnes, A. Dereux, and T. W. Ebbesen, Surface plasmon subwavelength optics, Nature (London) **424**, 824 (2003).

[5] S. Maier, *Plasmonics: Fundamentals and Applications* (Springer, New York, 2007).

[6] D. Sarid and W. A. Challener, *Modern Introduction to Surface Plasmons: Theory, Mathematica Modeling, and Applications* (Cambridge University, Cambridge, 2010).

[7] M. S. Tame, K. R. McEnery, S. K. Özdemir, J. Lee, S. M. Maier, and S. Kim, Quantum plasmonics, Nat. Phys. **9**, 329 (2013).

[8] A. Kamli, S. A. Moiseev, and B. C. Sanders, Coherent control of low loss surface polaritons, Phys. Rev. Lett. **101**, 263601 (2008).

[9] S. A. Moiseev, A. A. Kamli, and B. C. Sanders, Low-loss nonlinear polaritonics, Phys. Rev. A **81**, 033839 (2010).

[10] C. Tan and G. Huang, Superluminal surface polaritonic solitons at weak light level via coherent population oscillation, Phys. Rev. A **89**, 033860 (2014).

[11] S. Asgarnezhad-Zorgabad, R. Sadighi-Bonabi, and B. C. Sanders, Excitation and propagation of surface polaritonic rogue waves and breathers, Phys. Rev. A **98**, 013825 (2018).

[12] S. Asgarnezhad-Zorgabad, Coherent amplification and inversion less lasing of surface plasmon polaritons in a negative index metamaterial with a resonant atomic medium, Sci. Rep. **11**, 3450 (2021).

[13] Z. Gu, Q. Liu, Y. Zhou, and C. Tan, Symmetric and antisymmetric surface plasmon polariton solitons in a metal-dielectric-metal waveguide with incoherent pumping, Eur. Phys. J. D **74**, 78 (2020).

[14] Y. Duan, S. Liu, and C. Tan, Electromagnetically induced grating of surface polaritons via coherent population oscillation, Photonics **9**, 697 (2022).

[15] S. L. McCall and E. L. Hahn, Self-induced transparency, Phys. Rev. **183**, 457 (1969).

[16] G. L. Lamb, Analytical descriptions of ultrashort optical pulse propagation in a resonant medium, Rev. Mod. Phys. **43**, 99 (1971).

[17] M. J. Ablowitz, D. J. Kaup, and A. C. Newell, Coherent pulse propagation, a dispersive, irreversible phenomenon, J. Math. Phys. **15**, 1852 (1974).

[18] J. H. Eberly, Area theorem rederived, Opt. Express **2**, 173 (1998).

[19] E. L. Hahn, N. S. Shiren, and S. L. McCall, Application of the area theorem to phonon echoes, Phys. Lett. A **37**, 265 (1971).

[20] R. Friedberg and S. R. Hartmann, Superradiant damping and absorption, Phys. Lett. A **37**, 285 (1971).

[21] S. A. Moiseev, Some general nonlinear properties of photon-echo radiation in optically dense media, Optika i Spektroskopiya **62**, 302 (1987) [Opt. Spectrosc. **62**, 180 (1987)].

[22] R. Urmancheev, K. Gerasimov, M. Minnegaliev, T. Chanelière, A. Louchet-Chauvet, and S. Moiseev, Two-pulse photon echo area theorem in an optically dense medium, Opt. Express **27**, 28983 (2019).

[23] S. A. Moiseev, M. Sabooni, and R. V. Urmancheev, Photon echoes in optically dense media, Phys. Rev. Res. **2**, 012026(R) (2020).

[24] S. Wang, L. Yang, M. Shen, W. Fu, Y. Xu, R. L. Cone, C. W. Thiel, and H. X. Tang, Er : LiNbO₃ with high optical coherence enabling optical thickness control, Phys. Rev. Appl. **18**, 014069 (2022).

[25] T. Chanelière, Strong excitation of emitters in an impedance matched cavity: The area theorem, π-pulse and self-induced transparency, Opt. Express **22**, 4423 (2014).

[26] S. A. Moiseev and R. V. Urmancheev, Photon/spin echo in a fabry-perot cavity, Opt. Lett. **47**, 3812 (2022).

[27] C. Greiner, T. Wang, T. Loftus, and T. W. Mossberg, Instability and pulse area quantization in accelerated superradiant atom-cavity systems, Phys. Rev. Lett. **87**, 253602 (2001).

[28] J. H. Eberly and V. V. Kozlov, Wave equation for dark coherence in three-level media, Phys. Rev. Lett. **88**, 243604 (2002).

[29] G. Shchedrin, C. O'Brien, Y. Rostovtsev, and M. O. Scully, Analytic solution and pulse area theorem for three-level atoms, Phys. Rev. A **92**, 063815 (2015).

[30] R. Gutiérrez-Cuevas and J. H. Eberly, Vector-soliton storage and three-pulse-area theorem, Phys. Rev. A **94**, 013820 (2016).

[31] S. A. Moiseev, Quantum memory for intense light fields based on the photon echo, Izvestiya Akademii Nauk. Rossijskaya Akademiya Nauk. Seriya Fizicheskaya **68**, 1260 (2004) [Bull. Russ. Acad. Sci. Phys. **68**, 1408 (2004)].

[32] S. A. Moiseev, M. M. Minnegaliev, E. S. Moiseev, K. I. Gerasimov, A. V. Pavlov, T. A. Rupasov, N. N. Skryabin, A. A. Kalinkin, and S. P. Kulik, Pulse-area theorem in a single-mode waveguide and its application to photon echo and optical memory in $Tm^{3+} : Y_3Al_5O_{12}$, Phys. Rev. A **107**, 043708 (2023).

[33] R. M. Arkhipov, M. V. Arkhipov, I. Babushkin, and N. N. Rosanov, Self-induced transparency mode locking, and area theorem, Opt. Lett. **41**, 737 (2016).

[34] A. Pakhomov, M. Arkhipov, N. Rosanov, and R. Arkhipov, Area theorem in a ring laser cavity, Phys. Rev. A **108**, 023506 (2023).

[35] V. Veselago, The electrodynamics of substances with simultaneously negative values of ϵ and μ, Sov. Phys. Usp. **10**, 509 (1968).

[36] J. B. Pendry, A. J. Holden, W. J. Stewart, and I. Youngs, Extremely low frequency plasmons in metallic mesostructures, Phys. Rev. Lett. **76**, 4773 (1996).

[37] V. Shalaev, Optical negative-index metamaterials, Nat. Photon. **1**, 41 (2007).

[38] M. C. Berrington, M. J. Sellars, J. J. Longdell, H. M. Rønnow, H. H. Vallabhapurapu, C. Adambukulam, A. Laucht, and R. L. Ahlefeldt, Negative refractive index in dielectric crystals containing stoichiometric rare-earth ions, Adv. Opt. Mater. **11**, 2301167 (2023).

[39] S. A. Uriri, T. Tashima, X. Zhang, M. Asano, M. Bechu, D. O. Güney, T. Yamamoto, Ş. K. Özdemir, M. Wegener, and M. S. Tame, Active control of a plasmonic metamaterial for quantum state engineering, Phys. Rev. A **97**, 053810 (2018).

[40] C. Li, P. Yu, Y. Huang, Q. Zhou, J. Wu, Z. Li, X. Tong, Q. Wen, H.-C. Kuo, and Z. M. Wang, Dielectric metasurfaces: From wavefront shaping to quantum platforms, Prog. Surf. Sci. **95**, 100584 (2020).

[41] N. Rivera and I. Kaminer, Light-matter interactions with photonic quasiparticles, Nat. Rev. Phys. **2**, 538 (2020).

[42] A. S. Solntsev, G. S. Agarwal, and Y. S. Kivshar, Metasurfaces for quantum photonics, Nat. Photon. **15**, 327 (2021).

[43] J. Liu, M. Shi, Z. Chen, S. Wang, Z. Wang, and S. Zhu, Quantum photonics based on metasurfaces, Opto-Electronic **4**, 200092 (2021).

[44] X. Zhang, Surface polaritons and their coupling with emitters in periodic structures, Ph.D. thesis, University of York, 2014.

[45] P. Törmä and W. L. Barnes, Strong coupling between surface plasmon polaritons and emitters: A review, Rep. Prog. Phys. **78**, 013901 (2014).

[46] J. J. Choquette, K.-P. Marzlin, and B. C. Sanders, Superradiance, subradiance, and suppressed superradiance of dipoles near a metal interface, Phys. Rev. A **82**, 023827 (2010).

[47] M. Gomez-Castano, A. Redondo-Cubero, L. Buisson, J. L. Pau, A. Mihi, S. Ravaine, R. A. L. Vallee, A. Nitzan, and M. Sukharev, Energy transfer and interference by collective electromagnetic coupling, Nano Lett. **19**, 5790 (2019).

[48] A. Blake and M. Sukharev, Photon echo in exciton-plasmon nanomaterials: A time-dependent signature of strong coupling, J. Chem. Phys. **146**, 084704 (2017).

[49] T. A. R. Purcell, M. Sukharev, and T. Seideman, Modeling optical coupling of plasmons and inhomogeneously broadened emitters, J. Chem. Phys. **150**, 124112 (2019).

[50] P. Goldner, A. Ferrier, and O. Guillot-Noël, *Handbook on the Physics and Chemistry of Rare Earths* (Elsevier, New York, 2015), Chap. 267, pp. 1–78.

[51] Z. Zhou, C. Liu, C. Li, G. Guo, D. Oblak, M. Lei, A. Faraon, M. Mazzera, and H. de Riedmatten, Photonic integrated quantum memory in rare-earth doped solids, Laser Photonics Rev. **17**, 2300257 (2023).

[52] M. Guo, S. Liu, W. Sun, M. Ren, F. Wang, and M. Zhong, Rare-earth quantum memories: The experimental status quo, Front. Phys. **18**, 21303 (2023).

[53] A. Salomon, R. J. Gordon, Y. Prior, T. Seideman, and M. Sukharev, Strong coupling between molecular excited states and surface plasmon modes of a slit array in a thin metal film, Phys. Rev. Lett. **109**, 073002 (2012).

[54] S. Huang, C. Song, G. Zhang, and H. Yan, Graphene plasmonics: Physics and potential applications, Nanophotonics **6**, 1191 (2017).

[55] V. N. Pustovit and T. V. Shahbazyan, Cooperative emission of light by an ensemble of dipoles near a metal nanoparticle: The plasmonic Dicke effect, Phys. Rev. Lett. **102**, 077401 (2009).

[56] R. F. Oulton, V. J. Sorger, T. Zentgraf, R.-M. Ma, C. Gladden, L. Dai, G. Bartal, and X. Zhang, Plasmon lasers at deep subwavelength scale, Nature (London) **461**, 629 (2009).

[57] V. G. Bordo, Dicke superradiance from a plasmonic nanocomposite slab, J. Opt. Soc. Am. B **38**, 2104 (2021).

[58] D.-G. Seo, S.-Y. Le, C.-W. Jung, D. Ahn, J.-H. Kim, W.-S. Han, and K.-J. Yee, Dynamics of surface-plasmon lasing in planar metal gratings on semiconductor, Opt. Express **31**, 16205 (2023).

[59] Rituraj, M. Orenstein, and S. Fan, Scattering of a single plasmon polariton by multiple atoms for in-plane control of light, Nanophotonics **10**, 579 (2021).

[60] S. A. Moiseev and E. S. Moiseev, in *Multi Mode Nano Scale Raman Echo Quantum Memory*, edited by J. Kowalik, R. Horodecki, and S. Y. Kilin (IOS Press, Amsterdam, 2010), Vol. 26, pp. 212–223.

[61] S. Hughes, Breakdown of the area theorem: Carrier-wave Rabi flopping of femtosecond optical pulses, Phys. Rev. Lett. **81**, 3363 (1998).

[62] L. Novotny and B. Hecht, *Nano-Optics* (Cambridge University, Cambridge, 2012).